RAY W. HERRICK LABORATORIES

A Graduate Research Facility
of The School of Mechanical Engineering

Purdue University

West Lafayette, Indiana 47907

(NASA-CR-173915) THE PREDICTION OF ACOUSTICAL PARTICLE MOTION USING AN EFFICIENT POLYNOMIAL CURVE FIT PROCEDURE Interim Report (Purdue Univ.) 54 p HC A04/MF A01 CSCL 20A G3/71

N84-33145

Unclas 01112

A STUDY OF METHODS TO PREDICT AND MEASURE THE TRANSMISSION OF SOUND THROUGH THE WALLS OF LIGHT AIRCRAFT

Research Contract #0226-52-1288

THE PREDICTION OF ACOUSTICAL PARTICLE MOTION USING AN EFFICIENT POLYNOMIAL CURVE FIT PROCEDURE

Sponsored by

NASA
Hampton, VA 22365

Report No. # #0226-13 HL 84-23

Submitted by:

Steven E. Marshall, Graduate Research Assistant
Robert Bernhard, Principal Investigator

Approved by:

Raymond Cohen, Director
Ray W. Herrick Laboratories

August 1984

CONTENTS

1. INTRODUCTION

A need presently exists for better low-frequency noise reduction techniques. The fundamental methods for noise attenuation such as transmission loss or absorption are good for high frequency noise but provide limited success at reducing low-frequency noise. Analytical approaches to noise control also prove more effective for evaluating high frequency noise than low frequency noise. In order to better evaluate and attenuate low frequency noise, new analysis techniques are needed.

A low frequency noise problem that often confronts noise control engineers in the transportation industries is cavity 'boom.' Cavity 'boom' is characteristic of an acoustic resonance condition. The resonance occurs primarily as the result of acousto-structural coupling between the cavity and a compliant portion of the enclosing structure. The structure by its motion excites one or more of the low order acoustic modes. The source of the excitation is inherently difficult to identify and evaluate.

Although the frequencies of the resonant modes in an acoustic cavity are determined by spectral analysis techniques, the character of the acoustic mode shapes is not currently obtained experimentally. For example, the two-microphone intensity method is ineffective for measurement in reactive fields. A knowledge of the mode shapes, in

particular in terms of the particle motion, is advantageous in selecting an optimum noise attenuation solution.

The primary objective for the research presented here is the development of a procedure whereby the acoustic modal parameters, natural frequencies and mode shapes, in the cavities of transportation vehicles are determined experimentally. Furthermore, it should be possible to describe the acoustic mode shapes in terms of the particle motion.

The well-known structural modal anlaysis techniques have long been adapted to mini-computer based dynamic analysis systems. A secondary objective for this study is to tailor the acoustic modal analysis procedure to existing mini-computer based spectral analysis systems.

2. ACOUSTIC THEORY

2.1 Dynamic System Identification

2.1.1 Frequency Response

Harmonic excitation is often encountered in engineering systems. Although pure harmonic excitation is less likely to occur than periodic or other types of excitation, understanding the behavior of a system undergoing harmonic excitation is essential in order to comprehend how the system will respond to more general types of excitation. Harmonic excitation may be in the form of a force or displacement at some point in the system.

The frequency response method is a harmonic analysis. A sinusoidal excitation is applied to a system and its steady-state response is examined over a frequency range of interest. For a linear system, both the excitation and the system response are sinusoidal of the same frequency. For a simple example, consider a damped, single degree-of-freedom system subject to harmonic excitation, Figure 1.

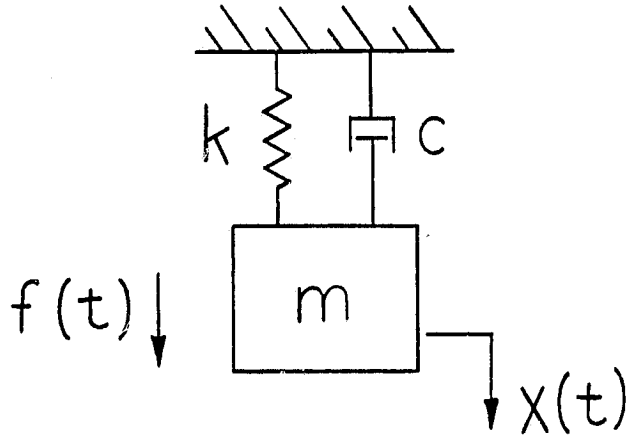

Figure 1. Single DOF System with Forcing Function

The second-order linear differential equation of motion is written as [1].

$$m\ddot{x}(t) + c\dot{x}(t) + kx(t) = f(t) \qquad 2.1$$

where the forcing function is given by

$$f(t) = \bar{F}_o e^{j\omega t} \qquad 2.2$$

The excitation frequency, ω, is sometimes referred to as the driving frequency. By substituting equation 2.2 into equation 2.1 and dividing by m, the equation of motion becomes

$$\ddot{x}(t) + 2\zeta\omega_n\dot{x}(t) + \omega_n^2 x(t) = \frac{1}{m}\bar{F}_o e^{j\omega t} \qquad 2.3$$

where

$$\omega_n = \sqrt{\frac{k}{m}} = \text{undamped natural frequency} \qquad 2.4$$

and

$$\zeta = \frac{c}{2m\omega_n} = \text{damping factor} \qquad 2.5$$

If a particular solution to equation 2.3 is assumed to be of the form

$$x(t) = \bar{X}e^{j\omega t} \qquad 2.6$$

an expression for the response is found to be

$$\bar{X} = \frac{\bar{F}_o/k}{1-(\omega/\omega_n)^2 + j2\zeta\omega/\omega_n} = Xe^{-j\Phi} \qquad 2.7$$

where

$$X = \frac{F_o/k}{\{[1-(\omega/\omega_n)^2]^2 + (2\zeta\omega/\omega_n)^2\}^{1/2}} \qquad 2.8$$

and

$$\Phi = \tan^{-1} \frac{2\zeta\omega/\omega_n}{1-(\omega/\omega_n)^2} \qquad 2.9$$

represent displacement amplitude and phase angle.

The excitation is given by the real part of f(t) [2]. Then, the response is given by the real part of x(t). Therefore, the response will be regarded as the real part of the complex quantity satisfying equation 2.3. Thus, the steady-state response is shown to be

$$x(t) = \mathrm{Re}\left[\frac{\bar{F}_o e^{j\omega t}/k}{1-(\omega/\omega_n)^2 + j2\zeta\omega/\omega_n}\right] \qquad 2.10$$

By evaluation of equation 2.10, it is seen that the response, x(t), is proportional to the force, f(t). The proportionality factor expressed in the frequency domain is given by

$$H(\omega) = \frac{1/k}{1-(\omega/\omega_n)^2 + j2\zeta\omega/\omega_n} \qquad 2.11$$

Equation 2.11 is known as the complex frequency response. The frequency response represents the ratio of the response to the excitation under steady-state conditions. Frequency response method is a mathematical mechanism for characterizing a dynamic system. It is noteworthy from equation

2.11 that if the driving frequency is near the natural frequency, the magnitude of the frequency response is limited only by the damping factor.

Detailed analysis of the frequency response for a damped, single degree-of-freedom system appears in the text and will not be addressed here [3].

2.1.2 Transfer Function

A fundamental concept employed by engineers for the purpose of characterizing a dynamic, linear system is that of system identification. As represented by the 'black box' analogy, the engineer by subjecting a system to a known input and recording the response can characterize the system. The mathematical model defining the input-output relationship of a physical system is termed the transfer function.

By transforming the system excitation and system response to a complex domain, denoted by the subsidiary variable s, an exact expression for the transfer function is obtained. If the system has a single input and single output, the transfer function can be represented by means of a block diagram as shown in Figure 2. When expressed in equation form,

$$X(s) = H(s)F(s) \qquad 2.12$$

the transfer function can be defined as an operator.

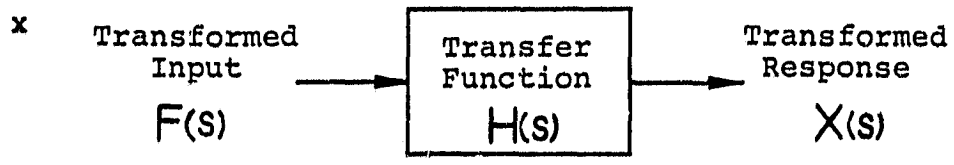

Figure 2. Block Diagram for a Transfer Function

In order to demonstrate the transfer function method for system characterization, consider the system defined in the previous section. If equation 2.3 is transformed to the Laplace domain, the following expression results:

$$s^2X(s) + 2\zeta\omega_n sX(s) + \omega_n^2 X(s) = \frac{1}{m} F(s) \qquad 2.13$$

The system transfer function is found by rearranging equation 2.13 to the form

$$H(s) = \frac{X(s)}{F(s)} = \frac{\frac{1}{m}}{s^2 + 2\zeta\omega_n s + \omega_n^2} \qquad 2.14$$

By substituting $j\omega$ for s in equation 2.14 and rearranging, the following expression is obtained,

$$H(\omega) = \frac{1/k}{1-(\omega/\omega_n)^2+j2\zeta\omega/\omega_n} \qquad 2.15$$

It is noteworthy that comparison of equations 2.15 and equation 2.11 prove them to be identical, the complex frequency response.

It is evident that the transfer function method is another technique to evaluate the frequency response data

of a system. The transfer function of a complex system can be determined from experimental data. Thus, a system can be identified by data from a frequency response test.

2.2 Modal Analysis

An alternative method for characterizing a system's dynamic behavior is by defining each of the system's component modes of vibration. A discrete dynamic system has as many natural frequencies and modes of vibration as degrees of freedom. The general motion of the system can be described by the superposition of the modes of vibration.

Modal analysis is defined as the process of characterizing the dynamics of a system in terms of its modes of vibration. Each mode is described in terms of three modal parameters: an undamped natural frequency, a measure of energy dissipation, damping, and a characteristic deflection shape, mode shape. A mode shape is a unique deformation shape that the system would acquire if excited solely at the frequency associated with that mode. Determination of the three modal parameters for the modes of a system is the task of modal analysis.

2.2.1 Analytical Modal Analysis

In order to mathemtically interpret the modal parameters, a simple structural model is analyzed. Consider a linear, undamped system of n degrees of freedom represented

by the differential equations of motion in matrix form [4],

$$[m]\{\ddot{x}(t)\} + [k]\{x(t)\} = \{0\} \qquad 2.16$$

If solutions to the equation are assumed to be of the form

$$x_i(t) = u_i e^{\lambda t} \qquad 2.17$$

and

$$\ddot{x}_i(t) = \lambda^2 u_i e^{\lambda t} = \lambda^2 x_i(t) \qquad 2.18$$

then by substituting into the equations of motion and rearranging, the following equation results:

$$[\lambda^2[m] + [k]]\{u\} = \{0\} \qquad 2.19$$

Equation 2.19 is a set of simultaneous algebraic equations in u, the unknowns being the u's and λ^2. For a nontrivial solution, $\{u\} \neq 0$, the determinant of the coefficients must equal zero. The determinant of the coefficients is a polynomial in λ^2. The roots of the polynomial are called the eigenvalues. If the eigenvalues are imaginary, then the modulus of the eigenvalues are equal to the natural frequencies of the system.

The solution vector, {u}, corresponding to a particular eigenvalue is termed an eigenvector. The eigenvectors are also referred to as modal vectors and represent physically a deformation pattern of the structure for a natural frequency of vibration. Since equation 2.19 is homogeneous, the solution for the eigenvectors is not unique. The vectors are unique only in the sense that the ratio between

any two elements in the vector is constant. Hence, the shape of the natural modes is unique, but not the amplitude. The process of adjusting the elements of the natural mode to render the amplitudes unique is normalization, and the resulting vectors are referred to as normal modes.

The natural modes satisfy a property called orthogonality. The statements of orthogonality with respect to the mass and stiffness matrices are as follows:

$$\{u\}_r^t[m]\{u\}_s = \{0\} \qquad 2.20$$

and

$$\{u\}_r^t[k]\{u\}_s = \{0\} \qquad 2.21$$

where r and s specify eigenvectors of different eigenvalue solution. The proof of the orthogonality of the modal vectors appears in the text and will not be demonstrated here [5].

The orthogonality property serves a useful purpose by allowing the equations of motion to be decoupled. For example, the modal matrix can be formed from the modal vectors in the form

$$[u] = [\{u\}_1\{u\}_2\ldots\{u\}_n] \qquad 2.22$$

The modal matrix functions to transform the mass and stiffness matrices to the generalized mass and stiffness matrices,

$$[u]^t[m][u] = [M] \qquad 2.23$$

and

$$[u]^t[k][u] = [K] \qquad 2.24$$

The generalized mass and stiffness matrices are both diagonal matrices due to the transformation.

If a new coordinate system is defined by the transformation

$$\{x\} = [u]\{q\} \qquad 2.25$$

then, substituting into equation 2.16, the equations of motion take the form

$$[m][u]\{\ddot{q}\} + [k][u]\{q\} = \{0\} \qquad 2.26$$

Pre-multiplying equation 2.26 by $[u]^t$ and substituting from equations 2.23 and 2.24 reduces the equations of motion to

$$[M]\{\ddot{q}\} + [K]\{q\} = \{0\} \qquad 2.27$$

Since the general mass and stiffness matrices are diagonal, the coordinate transformation has completely decoupled the equations of motion. Each equation in equation 2.27 is equivalent to a single degree of freedom and is easily solved by the method of Section 2.1.1.

The process of reducing a set of coupled system equations to an uncoupled set by coordinate transformation and performing analysis in the modal space from an nalytical sense is known as modal analysis. The same mathematical principles can be applied to systems with forcing functions or damping. When the damping is proportional to mass and

stiffness, the resulting coordinate transformation results in a set of uncoupled force response relationships exactly of the form of equation 2.3.

2.2.2 Experimental Modal Analysis

With the advent of the digital computer and the introduction of an efficient Fourier integral algorithm in 1965, experimental modal analysis has evolved into a frequently used and important engineering analysis tool. The theory governing structural modal analysis will be briefly reviewed as background for application to acoustical modal analysis.

Recalling the damped, single degree of freedom system from Section 2.1, it can be demonstrated that the transfer function, equation 2.14, can be rewritten to the form

$$H(s) = \frac{1/m}{(s-d)(s-d^*)} \qquad 2.28$$

where d represents the pole of the transfer function and is given by

$$d = \zeta\omega_n \pm j\omega_n\sqrt{1-\zeta^2} \qquad 2.29$$

and * is the complex conjugate operator [6]. Expanding equation 2.28 in partial fraction form results in

$$H(s) = \frac{1/m}{(s-d)(s-d^*)} = \frac{R_1}{(s-d)} + \frac{R_2}{(s-d^*)} \qquad 2.30$$

The residues of the transfer function are defined by the constants R_1 and R_2. The residues are directly related to

the amplitude of the response function. It is found by solving equation 2.31 that R_1 and R_2 are a complex conjugate pair. Thus, equation 2.30 becomes

$$H(s) = \frac{R}{(s-d)} + \frac{R^*}{(s-d^*)} \qquad 2.31$$

The concepts of poles and residues associated with a transfer function are integral to experimental modal analysis and will be recalled later.

An alternate method for determining the mode shapes from the eigenvalue problem of the previous section is by the use of an adjoint matrix [7]. If equation 2.19 can be reformulated to the expression given by

$$\left[[k]^{-1}[m]-\lambda^2[I]\right]\{u\} = \{0\} \qquad 2.32$$

then an additional matrix is defined by

$$[B(\lambda)] = \left[[k]^{-1}[m] - \lambda^2[I]\right] \qquad 2.33$$

From the identities

$$[B(\lambda)][B(\lambda)]^{-1} = [I] \qquad 2.34$$

and

$$[B(\lambda)]^{-1} = \frac{[C(\lambda)]}{|B(\lambda)|} \qquad 2.35$$

where $[(C(\lambda)]$ is the adjoint of matrix $[(B(\lambda)]$, the eigenvalue problem for solution, r, takes the form

$$[B(\lambda_r)][C(\lambda_r)] = |B(\lambda_r)|[I] \qquad 2.36$$

If λ_r^2 is a root of the characteristic equation 2.32, then

$$|B(\lambda_r)| = 0 \tag{2.37}$$

and equation 2.36 becomes

$$[B(\lambda_r)][C(\lambda_r)] = [0] \tag{2.38}$$

Rewriting equation 2.38 using only the j-th column of $[C(\lambda_r)]$ yields the equation

$$[B(\lambda_r)]\{C(\lambda_r)\}_j = \{0\} \tag{2.39}$$

Equation 2.39, like equation 2.32, represents a set of homogeneous equations in u which determine each value to within an arbitrary constant. Thus, vector $\{C(\lambda_r)\}_j$ and {u} are proportional and represent the mode shape associated with the eigenvalue r determined from the characteristic equation.

Similarly, consider the Laplace transform of equation 2.16 with the addition of forcing functions

$$\left[[m]s^2 + [k]\right]\{X(s)\} = \{F(s)\} \tag{2.40}$$

By substituting

$$[B(s)] = \left[[m]s^2 + [k]\right] \tag{2.41}$$

into equation 2.40, the equations of motion become

$$[B(s)]\{X(s)\} = \{F(s)\} \tag{2.42}$$

where [B(s)] is referred to as the system matrix. Premultiplying equation 2.42 by $[B(s)]^{-1}$ yields

$$[B(s)]^{-1}\{F(s)\} = \{X(s)\} \tag{2.43}$$

By specifying the relationship between the transfer

function matrix and the system matrix,

$$[H(s)] = [B(s)]^{-1} = \frac{[C(s)]}{|B(s)|} \qquad 2.44$$

the system responses are related to the system forcing functions through the transfer function matrix. Evaluating the adjoint matrix for the eigenvalues determined from the characteristic equation, it is apparent that the transfer function matrix contains both the eigenvalues and the eigenvectors to a proportionate constant.

The method for uncoupling the equations of motion by the adjoint matrix when applied to systems with proportionate damping results in the same adjoint matrix as for the undamped system. The poles of the characteristic equation are no longer the undamped natural frequencies, however, and are given in the form of equation 2.29.

The transfer function matrix is represented in the form [8]

$$\begin{bmatrix} H_{11}(s) & H_{21}(s) & H_{m1}(s) \\ H_{12}(s) & H_{22}(s) & H_{m2}(s) \\ H_{1m}(s) & H_{2m}(s) & H_{mm}(s) \end{bmatrix} \qquad 2.45$$

where m is the number of degrees-of-freedom. Substituting equation 2.45 into equation 2.43 and multiplying through yields

$$H_{11}(s)F_1(s) + \ldots + H_{1m}(s)F_m(s) = X_1(s) \qquad 2.46$$

$$H_{m1}(s)F_1(s) + \ldots + H_{mm}(s)F_m(s) = X_m(s)$$

If in equations 2.46 all forcing functions are set to zero except $F_1(s)$, then the individual transfer functions become

$$H_{11}(s) = \frac{X_1(s)}{F_1(s)} \qquad 2.47$$

$$H_{21}(s) = \frac{X_2(s)}{F_1(s)}$$

$$H_{m1}(s) = \frac{X_m(s)}{F_1(s)}$$

Thus, the first column of the transfer function matrix relates the response at all m degrees-of-freedom to an excitation at degree-of-freedom 1. It is noteworthy that all the individual transfer functions have the same characteristic equation.

Each of the transfer functions in equation 2.45 can be represented as the sum of the transfer functions for single degree-of-freedom systems in the form of equation 2.31,

$$H_{ab}(s) = \sum_{r=1}^{n} \left[\frac{R_r(a,b)}{(s-d_r)} + \frac{R_r^*(a,b)}{(s-d_r^*)} \right] \qquad 2.48$$

where $H_{ab}(s)$ relates the response at degree-of-freedom a to an excitation at degree-of-freedom b, and n is the number of roots to the characteristic equation. Thus, any of the transfer functions in equation 2.47 can be used to find the complex poles of equation 2.48. The transfer function matrix is now expressed in the form

$$[H(s)] = \sum_{r=1}^{n} \left[\frac{[R_r]}{(s-d_r)} + \frac{[R_r^*]}{(s-d_r^*)} \right] \qquad 2.49$$

Comparing equation 2.49 and equation 2.44, it is apparent that the residue matrix is equivalent to the adjoint matrix. From the definition of the system adjoint matrix, the residue matrix, $[R_r]$, evaluated at the natural frequencies is proportional to the mode shapes by the relationship

$$[R_r] = \alpha_r \{u_r\}\{u_r\}^t \qquad 2.50$$

Thus, each column of the residue matrix evaluated at the natural frequencies is proportional to the eigenvectors. The three modal parameters , ω_r, ζ_r, and u_r, are found from a single row or column of the transfer function matrix.

2.3 Acoustical Modal Analysis

2.3.1 Literature Survey

The analytical and experimental study of reactive acoustic fields and resonant modes has progressed, and record exists in the literature. A survey of recent developments will contribute to defining the direction of this research.

In some early work, Gladwell applied variational principles to formulate certain acoustical and structural configurations [9]. Later, Craggs considered variational statements in the context of finite element representations for the coupled structural-acoustic problem [10]. A comprehensive structural-acoustic theoretical model was

developed for interior sound fields using modal procedures by Dowell, Gorman, and Smith [11]. The sound fields which are created by arbitrary wall motions were modelled using Green's Theorem. Petyt, Lea, and Koopmann developed a finite element method for determining the acoustic modes of irregular cavities [12]. In the same time period, Wolf, Nefske, and Howell combined Dowell's modal procedures with both structural and acoustic finite element analysis to study automobile passenger compartments [13].

The finite element method lends itself readily to the acoustic problem, and many engineering problems are being analyzed by this method. Finite element modeling does, however, suffer two major disadvantages. Most acoustic finite element computer programs are very large in size, and thus require large computers with ample memory in which to operate. In order to obtain the required accuracy, models containing several thousand degrees-of-freedom are not uncommon. A second disadvantage of finite element modeling is the error due to the use of an inadequate number of elements or unrealistic boundary conditions.

It is particularly true in structural analysis that frequency response can be closely approximated using a truncated set of the total set of modes (usually the lower frequency modes). By using the procedures of equations 2.24 through 2.28, a significantly smaller approximate model can be developed. Thus, modal analysis where

acoustic and/or structural modes are found either experimentally or analytically and coupled to build an overall structural-acoustic modal model are very popular.

The technology for experimental modal analysis of acoustic fields is lagging both finite element modeling and experimental structural modal analysis. The majority of the research performed has been for the one-dimensional problem. Ibrahim and Mikulcik devised an experimental technique by which standing wave parameters in gas piping systems could be identified in the time domain [14]. Two pressure taps were made in an impedance tube. The tube was closed at one end and excited by a sweeping sine wave at the opposite end. The modal parameters were computed from the decay rates and amplitude ratios between the microphones. Experimental results agreed well with the theoretical results obtained from the undamped, plane wave equation.

A technique for experimental modal analysis of cavities involving Fourier analysis was proposed by Smith [15]. Evaluation of a one-dimensional tube with a small volume velocity source as the input showed that the response sound pressure is in-phase with the source volume velocity only at a cavity resonant frequency. Smith determined the acoustic pressure mode shapes by measuring transfer functions for several microphone locations and plotting the magnitude and phase at each resonant frequency.

In the results of a recent study, Mehl contended that background noise in pressure mode shape measurements was significant [16]. Mehl described numerical techniques for eliminating the effects of background noise in precise measurements of normal mode frequencies and damping. Resonant standing wave measurements were fitted to theoretical resonance formulas.

Neiter and Singh describe an acoustic modal analysis experiment employing existing software for structural modal analysis [17]. They describe the inherent characteristics of the acoustic system in terms of an acoustic impedance matrix, Z, by the relationship,

$$\{\bar{p}(s)\} = [\bar{Z}(s)]\{\bar{Q}(s)\} \qquad 2.51$$

where $\bar{Q}$ is the complex volume velocity source and $\bar{p}$ is the complex pressure response. By curve-fitting the measured impedance matrix to a frequency response function similar to equation 2.48, the modal parameters were extracted. The experimental results agreed well with a theoretical model possessing no damping.

In a report for research performed at Ray W. Herrick Laboratories, Byrne describes a procedure for experimentally determining, in terms of particle motions, the shapes of the low-order acoustic modes in three-dimensional enclosures [18]. Transfer functions were measured relating acoustic pressure response at an array of points in the

enclosure to a volume velocity source. The pressure mode shapes were described discretely by the peak amplitudes extracted from the transfer functions. A differentiable function was curve-fit to the discrete pressure amplitudes. The gradients of each approximate pressure mode function are determined and related to particle motion by the inviscid force equation,

$$\rho_o \frac{\partial \bar{u}}{\partial t} = -\nabla p \qquad 2.52$$

Thus, Byrne was able to describe the acoustic mode shapes in terms of particle motion.

2.3.2 Research Direction

The primary objective for the research presented here is the development of a procedure by which the three-dimensional modal response of an acoustic cavity is determined experimentally. It is advantageous to describe the acoustic mode shapes in terms of particle motion for excitation source identification. In light of the research survey presented in the previous section, the existing technology founded on the theory of modal analysis will be applied to the objectives. In this section, the research direction for application to the objectives is outlined.

A method for extracting the modal parameters of a mechanical system from the complex frequency response matrix is outlined in the first two sections. The system displacement response is related to the forcing functions

by the system matrix as given in equation 2.42. The analogous acoustical relationship for determining the complex pressure response due to a volume velocity source is expressed by equation 2.51. By assuming a lightly damped system, decoupled modes, and no background noise, the modal vectors are obtained directly from the residues of the measured frequency response functions.

The frequency response method assumes a lumped parameter system with a modal vector element for each degree of freedom. The mode shapes associated with the natural frequencies of a continuous system, however, are waveforms. For an acoustic system the waveforms correspond to standing waves. When the frequency response method is applied to continuous systems, the modal vectors become a discrete representation of the waveform deflection shapes. A function which approximates the mode shapes is obtained by performing a curve-fit procedure to the modal vectors. In acoustics, if the approximate pressure mode shape function is differentiable in space, then the mode shapes can be described in terms of particle motion by the inviscid force equation, equation 2.52.

In order to satisfy the objective for the development of an acoustic modal analysis procedure, the directions for research are outlined. The structural modal analysis systems commonly in use are all-inclusive mini-computer based systems. An additional research objective to be considered

is to tailor the acoustic modal analysis procedure including the curve-fit technique and graphic display to a minicomputer based spectral analysis system. The objective is accomplished by minimizing computation and storage space. Thus, the development of the acoustic modal analysis procedure will be performed on an existing spectral analysis system.

2.3.3 Theoretical Model

A theoretical model provides a reference for developing and verifying the acoustic modal analysis procedure. The model is obtained from solutions to the well-known acoustic wave equation, expressed in vector notation in terms of acoustic pressure as follows [19]:

$$\nabla^2 p = \frac{1}{c^2} \frac{\partial^2 p}{\partial t^2} \qquad 2.53$$

Equation 2.53 is the linearized, lossless wave equation for the propagation of sound in fluids. The general harmonic solution to the wave equation is of particular interest. If a solution in three-dimensional Cartesian coordinates of the form,

$$p(x,y,z,t) = F(x,y,z)e^{\lambda t} \qquad 2.54$$

is substituted into equation 2.53, then by a separation of variables procedure the solution is found to be [20]

$$p(x,y,z,t) = X(x)Y(y)Z(z)e^{\lambda t} \qquad 2.55$$

where

$$X(x) = A \cos k_x x + B \sin k_x x \qquad 2.56$$

$$Y(y) = C \cos k_y y + D \sin k_y y$$

$$Z(z) = E \cos k_z z + F \sin k_z z$$

In order to model an acoustic cavity, it is necessary to specify the domain boundary conditions. Acoustic cavity resonances are indicative of boundaries of relatively high acoustic impendance. For the free response problem, the acoustic cavity is assumed to be of dimensions L_x by L_y by L_z with orthogonal boundaries of infinite acoustic impendance located on the major axes and at L_x, L_y, and L_z. By fundamental acoustic principles at the boundaries,

$$n \cdot \bar{u} = 0 \qquad 2.57$$

$$n \cdot \nabla p = 0 \qquad 2.58$$

Thus, the boundary conditions bec me

$$\left(\frac{\partial p}{\partial x}\right)_{x=0,L_x} = 0 \qquad 2.59$$

$$\left(\frac{\partial p}{\partial y}\right)_{y=0,L_y} = 0$$

$$\left(\frac{\partial p}{\partial z}\right)_{z=0,L_z} = 0$$

When the boundary conditions are applied to the general harmonic solution, the following expession results

$$p_{lmn}(x,y,z,t) = P_{lmn} \cos \frac{l\pi x}{L_x} \cos \frac{m\pi y}{L_y} \cos \frac{n\pi z}{L_z} e^{\lambda_{lmn} t} \qquad 2.60$$

The symbol λ represents the eigenvalues, and the coefficient, P_{lmn}, is complex. The absolute value of imaginary eigenvalues are equal to the natural frequencies and are given by the relationship

$$|\lambda| = \omega_{lmn} = c\pi\left[\left(\frac{l}{L_x}\right)^2 + \left(\frac{m}{L_y}\right)^2 + \left(\frac{n}{L_z}\right)^2\right]^{1/2} \qquad 2.61$$

where l, m, and n are the respective mode numbers.

The solutions to the theoretical model, given by equation 2.60, represent three-dimensional standing waves in a rectangular cavity. In order to characterize the system by modal analysis techniques, the response is expressed as the sum of the individual pressure mode shapes in the form

$$p(x,y,z,t) = \sum_{l=0}^{\infty}\sum_{m=0}^{\infty}\sum_{n=0}^{\infty} P_{lmn} \cos\frac{l\pi x}{L_x} \cos\frac{m\pi y}{L_y} \cos\frac{n\pi z}{L_z} e^{\lambda_{lmn}t} \qquad 2.62$$

By determining the gradient of the individual pressure mode functions with respect to the three coordinate directions, the particle acceleration associated with the respective pressure mode is found via the inviscid force equation, equation 2.52. The gradient operator in Cartesian coordinates is given by

$$\nabla = \frac{\partial}{\partial x} + \frac{\partial}{\partial y} + \frac{\partial}{\partial z} \qquad 2.63$$

The partial derivative of the pressure mode function, equation 2.60, with respect to the x coordinate is found to be

$$\frac{\partial p}{\partial x} = \left(\frac{-L_x}{l\pi}\right) P_{lmn} \sin \frac{l\pi x}{L_x} \cdot$$

$$\cos \frac{m\pi y}{L_y} \cos \frac{n\pi z}{L_z} e^{\lambda_{lmn} t} \qquad 2.64$$

The partial derivatives of the pressure mode function with respect to the y and z coordinates are found similarly.

3. CURVE-FIT TO THREE-DIMENSIONAL DISCRETE DATA

From the frequency response method presented in the previous section, the modal vectors are obtained directly from the residues of the frequency response functions. The modal vectors resulting from the acoustic modal analysis procedure established in Section 2.3.2 discretely represent three-dimensional pressure standing waves. Functions which approximate the acoustic mode shapes are obtained by performing a curve-fit in space to the modal vectors. In this section a procedure for fitting a function to three-dimensional discrete data is developed.

An objective for the acoustic modal analysis procedure is to describe the acoustic mode shapes in terms of particle motion. From the previously cited inviscid force equation, it was established that the acceleration of a gas particle is given by the negative of the gradient of the pressure field at the location of the particle. Therefore, the particle acceleration mode shapes are obtained if the acoustic pressure mode shapes are described by a differentiable function. An objective for the curve-fit procedure is to derive an approximate pressure mode function which is differentiable with respect to the spatial coordinates.

The character of the acoustic mode shapes in an enclosure is directly dependent on the dimensional shape of the cavity and the surface boundary conditions. Thus, the most

that can be assumed concerning the pressure function describing an acoustic mode in an enclosure is that the shape is sinusoidal in space, due to the physical nature of sound. In addition, each data point in the modal vector is subject to experimental error which, for acoustic measurement, may be relatively large in magnitude. It is inappropriate to match an interpolating function exactly at the data points since no implicit assumption can be made concerning the accuracy of the data. The pressure mode function, therefore, must be assumed arbitrary. Thus, the objective is to find the 'best' curve which represents data that are subject to error. The criterion for goodness of fit is to some degree arbitrary, although the least squares criterion is most common and will be applied to the acoustic problem. The least squares procedure offers the benefit of a polynomial interpolating function which is numerically differentiable.

3.1 Least Squares Procedure

In order to define a three-dimensional acoustic domain, the Cartesian axes system is specified for this study. Thus, the function describing the acoustic pressure field associated with the r^{th} acoustic mode in an enclosure is $p_r(x,y,z)$. The procedure objective is to derive an approximate function to $p_r(x,y,z)$ which is differentiable with respect to the spatial coordinates. If the approximating function is specified to be $h_r(x,y,z)$, then the

following relationship holds

$$p_r(x,y,z) = h_r(x,y,z) + e(x,y,z) \qquad 3.1$$

The term e(x,y,z) represents error associated with the fit.

The least squares procedure developed by Gauss can be stated verbally as, 'the sum of the squares of the residuals of the differential equations should be minimum at the correct solution' [21]. The least squares error norm expressed mathematically for a function in three dimensions is as follows [22]

$$\|e\|_2 = \iiint e(x,y,z)^2 dxdydz \qquad 3.2$$

where from equation 3.1

$$e(x,y,z) = p_r(x,y,z) - h_r(x,y,z) \qquad 3.3$$

It is now necessary to expand the approximating function into a series of interpolating functions and constants

$$h_r(x,y,z) = c_1\Phi_1(x,y,z) + \ldots + c_i\Phi_i(x,y,z) \qquad 3.4$$

where i represents the order of the function. The error term is now given by

$$e(x,y,z) = p_r(x,y,z) - c_1\Phi_1(x,y,z) - \ldots - c_i\Phi_i(x,y,z) \qquad 3.5$$

and the least squares error norm becomes

$$\|e\|_2 = \iiint [p_r - c_1\Phi_1 - \ldots - c_i\Phi_i]^2 dxdydz \qquad 3.6$$

In order to complete the least squares procedure and minimize the error associated with the curve fit, the

partial derivative of equation 3.6 with respect to each constant is determined and set to zero

$$\partial \|e\|/\partial c_1 = 0 = \iiint 2[p_r - c_1\Phi_1 - \ldots - c_i\Phi_i](-\Phi_1)dxdydz \quad 3.7$$

$$\partial \|e\|/\partial c_i = 0 = \iiint 2[p_r - c_1\Phi_1 - \ldots - c_i\Phi_i](-\Phi_i)dxdydz$$

Equation 3.7 can be reduced to the form

$$\iiint p_r\Phi_1 dxdydz = c_1\iiint\Phi_1^2 dxdydx + \ldots + c_i\iiint\Phi_1\Phi_i dxdydz \quad 3.8$$

$$\iiint p_r\Phi_i dxdydz = c_1\iiint\Phi_i\Phi_1 dxdydz + \ldots + c_i\iiint\Phi_i^2 dxdydz$$

Equations 3.8 are rearranged to matrix form as

$$\begin{bmatrix} \iiint\Phi_1^2 dxdydz & \iiint\Phi_1\Phi_i dxdydz \\ x & x \\ \iiint\Phi_i\Phi_1 dxdydz & \iiint\Phi_i^2 dxdydz \end{bmatrix} \begin{Bmatrix} c_1 \\ x \\ c_i \end{Bmatrix} = \begin{Bmatrix} \iiint p_r\Phi_1 dxdydz \\ x \\ \iiint p_r\Phi_i dxdydz \end{Bmatrix} \quad 3.9$$

By solving equations 3.9 for the constants and substituting those valves into equation 3.4, the function, $h_r(x,y,z)$, has been determined which 'best' approximates the curve of the discrete data with respect to the least squares error norm.

3.2 Legendre Polynomials

A critical element in the least squares procedure is specifying the interpolating function to approximate the acoustic pressure mode function. In order to select the type of function most appropriate to the application, it is necessary to consider some important criteria:

a. The accuracy of the approximation is directly dependent on how well the polynomial function can approximate acoustic data as evaluated by some error norm. It is noteworthy that acoustic phenomena are sinusoidal in nature.

b. In order to solve the matrix equations for the constants of the polynomials, the polynomial function must be integrated with respect to the spatial coordinates. The ease at which the integration is performed becomes a key element of the procedure.

c. Recalling the objectives from the introduction, the acoustic modal analysis procedure should be tailored to mini-computers. Therefore, computation efficiency is greatly desired.

After a review of the available polynomial shape functions conducive to the least squares procedure, Legendre polynomials are selected for approximating the acoustic data. With reference to the aforementioned criteria, the selection was made on the following premise:

a. All complete interpolating polynomial families of sequential n^{th} order will approximate a sinusoidal function with equivalent accuracy. Thus, no accuracy is sacrificed by the use of Legendre polynomials over another interpolating polynomial.

b. Legendre polynomials are separable with respect to the three spatial coordinates. Therefore, the polynomial elements are integrated with respect to the associated spatial coordinates rather than being integrated over a unit volume element.

c. Legendre polynomials are orthonormal in the range from -1 to 1. The significance of this characteristic is that if all functions of interest to the least squares procedure are defined on the region -1 to 1, then all off-diagonal terms of the left-side matrix become zero. Thus, a considerable reduction in computation time has been attained.

The Legendre polynomials are listed as follows [23]:

$$S_o(u) = 1 \qquad S_3(u) = 1/2(5u^3-3u)$$

$$S_1(u) = u \qquad S_4(u) = 1/8(35u^4-30u^2+3) \qquad 3.10$$

$$S_2(u) = 1/2(3u^2-1) \qquad S_5(u) = 1/8(63u^5-70u^3+15u)$$

$$S_n(u) = \frac{2n-1}{n} uS_{n-1}(u) - \frac{n-1}{n} S_{n-2}(u)$$

In order to approximate a function of three-dimensions, it is necessary to create shape functions which are a product of three Legendre polynomials in the form

$$\Phi_i(x,y,z) = S_{lx}(x)S_{my}(y)S_{nz}(z) \qquad 3.11$$

where l,m,n represent the polynomial order in the respective directions. The maximum order required for the Legendre polynomials in the three directions is an important consideration and will be addressed in a subsequent section. The order of the shape function, i, is dependent on the order of the three Legendre polynomials and becomes a matter of bookkeeping when programmed in FORTRAN.

Recalling that Legendre polymonials are orthonormal in the region -1 to 1, the three dimensional acoustic domain must be mapped to a 2 x 2 x 2 cubic element in the ζ, η, ξ domain. As a result of the Legendre polynomials being separable with respect to the three coordinate directions, and since the acoustic domain is defined on an orthogonal axes system, the map reduces to merely a scaling in each of the three directions. The scale factors only become important when determining the gradient of the approximation function. The matrix equation, equation 3.9, is now transformed to

$$\begin{Bmatrix} \int_{-1}^{1}\int_{-1}^{1}\int_{-1}^{1} \Phi_l^2(\zeta,\eta,\xi)\,d\zeta d\eta d\xi & 0 \\ 0 & \int_{-1}^{1}\int_{-1}^{1}\int_{-1}^{1} \Phi_i^2(\zeta,\eta,\xi)\,d\zeta d\eta d\xi \end{Bmatrix} \begin{Bmatrix} c_l \\ x \\ c_i \end{Bmatrix} = \begin{Bmatrix} \int_{-1}^{1}\int_{-1}^{1}\int_{-1}^{1} p_r \Phi_l(\zeta,\eta,\xi)\,d\zeta d\eta d\xi \\ x \\ \int_{-1}^{1}\int_{-1}^{1}\int_{-1}^{1} p_r \Phi_i(\zeta,\eta,\xi)\,d\zeta d\eta d\xi \end{Bmatrix} \qquad 3.12$$

Computation can be further reduced by modifying the left side matrix in order to create the identity matrix. By obtaining the identity matrix from the left side of the equation, the constants, c_i, are solved for directly. An analysis of Legendre polynomials reveals that if the square of the polynomial is integrated exactly over the limits -1 to 1, a number results with a value directly associated with the order of the polynomial

$$\int_{-1}^{1} S_n(u)^2 du = 2/2n+1 \qquad 3.13$$

Thus, a series of constants can be defined to compliment the respective shape functions

$$\int_{-1}^{1}\int_{-1}^{1}\int_{-1}^{1} \Phi_i^2 d\zeta d\eta d\xi = \int_{-1}^{1}\int_{-1}^{1}\int_{-1}^{1} [S_{a\zeta}(\zeta) S_{b\eta}(\eta) S_{c\xi}(\xi)]^2 d\zeta d\eta d\xi$$

$$= (2/2a+1)(2/2b+1)(2/2c+1) = \rho_i \qquad 3.14$$

When both sides of the matrix equation 3.12 are divided by the constants, ρ_i, the left side matrix becomes the identity matrix, and the right side vector acquires the reciprocal of the normalizing constant

$$\begin{Bmatrix} 1 & 0 \\ x & x \\ 0 & 1 \end{Bmatrix} \begin{Bmatrix} c_1 \\ x \\ c_i \end{Bmatrix} = \begin{Bmatrix} 1/\rho_1 \int_{-1}^{1}\int_{-1}^{1}\int_{-1}^{1} p_r \Phi_1(\zeta,\eta,\xi) d\zeta d\eta d\xi \\ 1/\rho_i \int_{-1}^{1}\int_{-1}^{1}\int_{-1}^{1} p_r \Phi_i(\zeta,\eta,\xi) d\zeta d\eta d\xi \end{Bmatrix} \qquad 3.15$$

3.3 Numerical Integration

The matrix equation derived by the least squares procedure has now reduced to a series of integral equations:

$$c_1 = 1/\rho_1 \int_{-1}^{1}\int_{-1}^{1}\int_{-1}^{1} p_r \Phi_1(\zeta,\eta,\xi)\,d\zeta\,d\eta\,d\xi \qquad 3.16$$

$$\vdots$$

$$c_i = 1/\rho_i \int_{-1}^{1}\int_{-1}^{1}\int_{-1}^{1} p_r \Phi_i(\zeta,\eta,\xi)\,d\zeta\,d\eta\,d\xi$$

The constants that yield the best curve fit with respect to the least squares norm can be solved for directly by performing the required integration. In order to adapt the curve fitting procedure to a computer, the computing structure requires that the integration be performed numerically. Several numerical integration methods are in existence. The criterion for the method of integration is again accuracy and efficiency of computation.

Consideration of the existing numerical methods of integration results in the selection of the Newton-Coates numerical integration formulas. The Newton-Coates integration equations have the general form [24]

$$\int_{x_0}^{x_n} f(x)dx = K_n h(w_{0n}f_0 + w_{1n}f_1 + \ldots + w_{nn}f_n) \qquad 3.17$$

where

K_n = the n-point scheme constant

h = the distance between points

f = the value of the function at the points

w = the weighting constants of the function valves

The accuracy of the integration can be maximized by applying the point scheme equation that coincides exactly with the number of recorded values of the function being integrated. Alternatively, a combination of Simpson's 1/3 rule, 3/8 rule, and the trapezoidal rule can be applied for integration over any number of points.

By applying the Newton-Coates formula, equations 3.16 become

$$c_1 = 1/\rho_1 \sum_{a=1}^{n\zeta} \sum_{b=1}^{n\eta} \sum_{c=1}^{n\xi} p_{rabc} \Phi_1(\zeta_a, \eta_b, \xi_c) w_a w_b w_c \qquad 3.18$$

$$\vdots$$

$$c_i = 1/\rho_i \sum_{a=1}^{n\zeta} \sum_{b=1}^{n\eta} \sum_{c=1}^{n\xi} p_{rabc} \Phi_i(\zeta_a, \eta_b, \xi_c) w_a w_b w_c$$

The numerical integration can now be performed, and the constants of the approximation polynomial function are solved for directly. The structure of the mathematical procedure lends itself readily to FORTRAN or BASIC programming on a mini-computer.

3.4 Error Analysis

An important consideration for the development and evaluation of the modal analysis procedure is the accuracy with which the computed pressure mode function approximates the discretely measured pressure mode shapes. Recalling that the pressure mode shapes are sinusoidal in space, three questions concerning accuracy of fit should be addressed:

a. What is the minimum polynomial order that sufficiently approximates a sine function of a given number of wavelengths?

b. How many data points per wavelength are required to adequately describe a sine function?

c. What is the error associated with a numerical integration?

An analysis of the curve-fitting procedure with respect to the three points of question will allow for the design of an optimal configuration.

In order to evaluate the accuracy of the numerical procedure, a known function is approximated and an error criterion is established. After consideration of the various error norms, a standard deviation error criterion was chosen for judging accuracy. This error norm was chosen due to the discrete nature of the data and ease of evaluation. The error norm expressed in equation form is [25]

$$\|e\| = \left[\sum_{i=1}^{n} \frac{(p_r(i)-h_r(i))^2}{n-1} \right]^{1/2} \qquad 3.19$$

3.4.1 Polynomial Order

In order to evaluate error as a function of polynomial order, the error due to a polynomial approximation must be segregated from error due to other variables. By assuming a function, p_r, and performing an exact integration of

equation 3.16, the approximate function, h_r, is computed independent of numerical integration error or number of data points.

Recalling from the theoretical model, the pressure mode shape for the ideal case in one dimension will be of the form

$$p_r(x) = \cos l\pi x/L_x \qquad 3.20$$

Equation 3.20 represents the one-dimensional pressure mode shapes defined for the domain $0 \leq x \leq L_x$. In order to compute the coefficients of the approximation function, L_x is set to 2 and Equation 3.16 is modified such that the limits of integration are 0 and 2. By substituting (u-1) for u in the Legendre polynomials, equation 3.10, the limits of integration can be adjusted appropriately. With substitution of equation 3.20 and the modified Legendre polynomials into equation 3.16 and exact integration, the approximation function can be found.

The approximation function was computed for the first four modes, l = 1,2,3,4, with approximation functions of up to and including eighth-order polynomials. The error associated with each case is evaluated for eleven sample points via equation 3.19, and the results are presented in Table 1. The results show that in the absence of integration error, the approximation improves with increasing polynomial order.

Table 1. Approximation Error Using an Exact Integration

Mode Number	Polynomial Order							
	1st	2nd	3rd	4th	5th	6th	7th	8th
1st	.775	.117	.117	4.7e-3	4.7e-3	3.e-5	8.e-5	7.5e-7
2nd	.775	.775	.283	.283	.033	.033	.0017	.0017
3rd	.775	.754	.754	.454	.454	.091	.091	.0088
4th	.775	.775	.71	.71	.607	.607	.173	.173

3.4.2 Numerical Integration

The coefficients for the approximation function result from the numerical integration in equation 3.18. In order to perform the computation, the pressure mode function for one-dimension, equation 3.20, is described in terms of discrete values distributed evenly along the x-axis. It is intuitively obvious that the approximation error will approach zero as the increment between points decreases and the integration approaches an exact integration as discussed in the last section. A study of the error as a function of the number of integration points for an idealized case, however, illustrates the sensitivity of the approximation technique to integration error. Such error may lend insight into the design of later experiments. Therefore, rather than assume to minimize increment between points which increases data collection time, computation, and data storage space, the number of data points is a variable in the analysis.

An inverse relationship between error and polynomial order was proven for an exact integration approximation. The polynomial order for the curve-fitting procedure must be limited, however, to the benefit of computation time. In addition, a polynomial approximation of a sine wave may behave peculiarly for low order polynomials due to numerical integration error. The polynomial order, therefore, is an important variable in the error analysis.

The coefficients of the approximation functions corresponding to each combination of data points, polynomial order, and wave number is computed via equation 3.18. The error associated with each approximation is determined for eleven points in equation 3.19. The results are recorded and tabulated in Tables 2, 3, 4, and 5.

The accuracy of the approximations are, in general, satisfactory. Certain trends in the error tables, however, are worth noting. The error is unacceptable for the cases of the polynomial order exceeding the number of integration points. A minimum of eleven integration points is required to adequately approximate a cos 1 1/2 wave (3rd mode). In addition, in order to approximate a cos 2 wave (4^{th} mode), greater than eleven integration points are required. Further evaluation of the error tables is performed for the design of the experiments.

3.5 Approximation Function Gradient

Resulting from the curve-fit procedure are polynomial functions which approximate the pressure fields associated with the acoustic modes in enclosures. From the inviscid force equation, equation 2.52, the acceleration of a gas particle is given by the negative of the gradient of the pressure field at the location of the particle. Thus, in order to describe the acoustic mode shapes in terms of particle motion, the gradient of the approximate pressure function must be determined.

Table 2. Integration Error for a One-Half Cosine Wave

Number of Data Points	Polynomial Order							
	1st	2nd	3rd	4th	5th	6th	7th	8th
3	.775	.151	.151	1.312	1.312	2.857	2.857	5.083
4	.775	.112	.112	.460	.460	2.428	2.428	3.629
5	.775	.118	.118	.122	.122	1.078	1.078	2.866
6	.775	.117	.117	.068	.068	.535	.535	2.178
7	.775	.116	.116	.004	.004	.161	.161	1.382
8	.775	.116	.116	.0038	.0038	.096	.096	.763
9	.775	.116	.116	.0048	.0048	.007	.007	.242
10	.775	.116	.116	.0048	.0048	.0045	.0045	.151
11	.775	.116	.116	.0047	.0047	.0001	.0001	.012

Table 3. Integration Error for a Full Cosine Wave

Number of Data Points	Polynomial Order							
	1st	2nd	3rd	4th	5th	6th	7th	8th
3	.888	.888	1.157	1.157	1.425	1.425	4.687	4.687
4	.801	.801	.403	.403	1.511	1.511	2.480	2.480
5	.772	.772	.276	.276	.704	.704	1.8	1.8
6	.773	.773	.255	.255	.260	.260	1.35	1.35
7	.775	.775	.295	.295	.336	.336	1.047	1.047
8	.775	.775	.290	.290	.201	.201	.472	.472
9	.775	.775	.282	.282	.032	.032	.510	.510
10	.775	.775	.282	.282	.025	.025	.304	.304
11	.775	.775	.282	.282	.035	.035	.076	.076

Table 4. Integration Error for 1 1/2 Cosine Wave

Number of Data Points	Polynomial Order							
	1st	2nd	3rd	4th	5th	6th	7th	8th
3	.775	.862	.862	1.081	1.081	2.874	2.874	5.078
4	.775	.775	.775	1.433	1.433	1.433	1.433	3.998
5	.775	.850	.850	.765	.765	1.33	1.33	1.58
6	.775	.788	.788	.480	.480	.870	.870	1.913
7	.775	.745	.745	.436	.436	.757	.757	1.330
8	.775	.748	.748	.395	.395	.261	.261	1.116
9	.775	.755	.755	.515	.515	.780	.780	1.502
10	.775	.754	.754	.489	.489	.466	.466	.604
11	.775	.753	.753	.447	.447	.145	.145	1.267

Table 5. Integration Error for a Double Cosine Wave

Number of Data Points	Polynomial Order							
	1st	2nd	3rd	4th	5th	6th	7th	8th
3	1.225	1.225	1.225	1.225	2.646	2.646	3.338	3.338
4	.801	.801	1.007	1.007	1.421	1.421	2.527	2.527
5	.938	.938	.848	.848	1.604	1.604	1.042	1.042
6	.820	.820	.755	.755	1.088	1.088	1.401	1.401
7	.770	.770	.913	.913	1.002	1.002	.974	.974
8	.769	.769	.778	.778	.617	.617	.731	.731
9	.778	.778	.705	.705	.733	.733	1.252	1.252
10	.777	.777	.702	.702	.529	.529	.437	.437
11	.774	.774	.717	.717	.851	.851	1.763	1.763

The approximate pressure function results from substituting the constant values obtained in equation 3.18 into the following equation:

$$h_r(\zeta,\eta,\xi) = c_1\Phi_1(\zeta,\eta,\xi) +\ldots+ c_i\Phi_i(\zeta,\eta,\xi) \qquad 3.21$$

It is noteworthy that the approximate pressure function is defined in the ζ, η, ξ domain. In order to obtain the particle acceleration for the original acoustic domain, defined in x, y, and z, the gradient of equation 3.21 with respect to x, y, and z must be computed. The partial derivative of equation 3.21 with respect to the x coordinate is found by the application of the chain rule as follows

$$\frac{\partial h_r(\zeta,\eta,\xi)}{\partial x} = \frac{\partial h_r}{\partial \zeta}\frac{\partial \zeta}{\partial x} + \frac{\partial h_r}{\partial \eta}\frac{\partial \eta}{\partial x} + \frac{\partial h_r}{\partial \xi}\frac{\partial \xi}{\partial x} \qquad 3.22$$

Since both the x, y, z domain axes and the ζ, η, ξ domain axes are orthogonal, x is not a function of η or ξ . Thus, $\frac{\partial \eta}{\partial x}$ and $\frac{\partial \xi}{\partial x}$ are zero. Furthermore, the term $\frac{\partial \zeta}{\partial x}$ is merely the constant ratio of the domain length along the ζ axes, 2, to the length of the acoustic domain in the x direction, L_x. The same properties hold true for the partial derivatives of equation 3.21 with respect to the y and z coordinates.

The variable terms resulting from the application of the chain rule to equation 3.21 represent the gradient of the approximate pressure function with respect to the ζ, η, and ξ coordinates. In order to compute the gradient, the

derivatives of equations 3.10, the Legendre polynomials, with respect to u are determined. By substituting equation 3.11 and equation 3.21 into equation 3.22, an expression for the partial derivative of the approximate pressure function results

$$\frac{\partial h_r(\zeta,\eta,\xi)}{\partial x} = \left[\sum_{j=1}^{i} c_j \frac{\partial S_{l\zeta}(\zeta)}{\partial \zeta} S_{m\eta}(\eta) S_{n\xi}(\xi)\right][2/L_x] \qquad 3.23$$

where l, m, and n represent the Legendre polynomial orders associated with the shape function order, j. Expressions for the partial derivatives of equation 3.21 with respect to the y and z coordintes are found similarly to be

$$\frac{\partial h_r(\zeta,\eta,\xi)}{\partial y} = \left[\sum_{j=1}^{i} c_j S_{l\zeta}(\zeta) \frac{\partial S_{m\eta}(\eta)}{\partial \eta} S_{n\xi}(\xi)\right][2/L_y] \qquad 3.24$$

and

$$\frac{\partial h_r(\zeta,\eta,\xi)}{\partial z} = \left[\sum_{j=1}^{i} c_j S_{l\zeta}(\zeta) S_{m\eta}(\eta) \frac{\partial S_{n\xi}(\xi)}{\partial \xi}\right][2/L_z] \qquad 3.25$$

Substitution of equations 3.23, 3.24, and 3.25 into the inviscid force equation yields an expression for the acoustic mode shapes in terms of particle acceleration. The numerical operations in the three equations are conducive to FORTRAN or BASIC programming.

4. CONCLUSIONS

The primary objective for the research presented here, as stated in the introduction, is the development of a procedure for experimentally determining the modal parameters associated with resonance conditions in the cavities of transportation vechicles. It is desirable for noise control diagnostics to describe the mode shapes in terms of particle motion. The acoustic modal analysis procedure should be adapted to function on existing computer based spectral analysis systems.

In general, the objectives for the research are satisfied. A procedure is developed whereby the acoustic mode shapes associated with the cavity resonances in an enclosure are determined experimentally and described in terms of particle motion. While not currently implemented on a mini-computer system, the modal analysis procedure including the curve-fitting program is constructed for use on small computer systems.

The curve-fitting program performed satisfactorily for the modal analysis experiments by approximating the pressure mode functions discretely described by the modal vectors. Several improvements to the curve-fitting procedure are suggested, however. The procedure is limited due to the error resulting from fitting to a relatively few points. The program should be expanded to accomodate a

larger number of data points. Furthermore, excessive error can result from extrapolating a polynomial function approximation of a sinusoid beyond the measurement domain. Either the acoustic pressure must be measured to the enclosing surfaces, or a shape function which approximates the harmonic acoustic pressure function beyond the measurement field should be introduced in the curve-fitting program. Finally, the requirement for equally spaced, orthogonal input data to the curve-fitting program hampers measurements in irregular shaped domains.

The task of data acquisition for the necessary number of points to adequately describe the acoustic modes in a typical transportation vehicle is long and tedious. Improved data collection techniques are a necessity. Two recommendations are for a microphone array attached to a multiple input spectrum analyzer or a stepper motor controlled point collection device.

5. REFERENCES

1. Thomson, W.T., Theory of Vibration. Prentice-Hall, Inc., New Jersey, 1972.

2. Meirovitch, L., Elements of Vibration Analysis. McGraw-Hill, Inc., 1975, page 42.

3. Tse, F.S., Morse, I.E., Hinkle, R.T., Mechanical Vibrations. Allyn and Bacon, Inc., Massachusetts, 1978.

4. Krousgrill, C., ME563 (Mechanical Vibrations) - classnotes. Purdue University, Fall Semester, 1982.

5. Meirovitch, L. Elements of Vibration Analysis. McGraw-Hill, Inc., 1975, pages 143-146.

6. Cruz, J.B., and Valkenburg, M.E., Signals in Linear Circuits. Houghton Mifflin Company, Boston, 1974.

7. Meirovitch, L., Analytical Methods in Vibrations. MacMillan Co., New York, 1967.

8. Brown, D.L., ME696 (Fourier Analysis)-classnotes. University of Cincinnati, Spring, 1979.

9. Gladwell, G.M., "A Variational Formulation of Damped Acousto-Structural Vibration Problems". Journal of Sound and Vibration, 1966, 4, 2.

10. Craggs, A., "The Transient Response of a Coupled Plate-Acoustic System Using Acoustic Finite Elements". Journal of Sound and Vibration, 1971, 15, 1.

11. Dowell, E.H., Gorman, G.F., Smith, D.A., "Acoustoelasticity: General Theory, Acoustic Natural Modes and Forced Response to Sinusoidal Excitation, Including Comparisons with Experiment". Journal of Sound and Vibration, 1977, 52, 4.

12. Petyt, M., Lea, J., Koopman, G.H., "A Finite Element Method for Determining the Acoustic Modes of Irregular Shaped Cavities". Journal of Sound and Vibration, 1976, 45, 3.

13. Wolf, J.A., Nefske, D.J., Howell, L.J., "Structural-Acoustic Finite Element Analysis of the Automobile Passenger Compartment". Society of Automotive Engineers, February 1976.

14. Ibrahim, S.R., Mikulcik, E.C., "Time Domain Identification of Standing Wave Parameters in Gas Piping Systems". Journal of Sound and Vibration, 1978, 60, 1.

15. Smith, D.L., "Experimental Techniques for Acoustic Modal Analysis of Cavities". Inter-noise, Washington, D.C., April 1976.

16. Mehl, J.B., "Analysis of Resonance Standing-Wave Measurements". J. Acoust. Soc. Am., November 1978, 64, 5.

17. Nieter, J.J., Singh, R., "Acoustic Modal Analysis Experiment". J. Acoust. Soc. Am., August 1982, 72, 2.

18. Byrne, K.P., "Experimental Determination of the Particle Motions Associated with the Low Order Acoustic Modes in Enclosures". Herrick Labs. Report for NASA, No. 5, HL 83-22.

19. Kinsler, L.E., Frey, A.R., Fundamentals of Acoustics. John Wiley and Sons, New York, 1976.

20. Crocker, M.J., ME513 (Engineering Acoustics)-classnotes. Purdue University, Fall Semester, 1982.

21. Kreyszig, E., Advanced Engineering Mathematics. John Wiley and Sons, New York, 1972.

22. Bernhard, R.J., ME597B (Finite Element Method)-classnotes. Purdue University, Spring Semester, 1983.

23. Spiegel, M., Mathematical Handbook, Schaum's Series. McGraw-Hill Book Co., New York, 1968.

24. Gerald, C., Applied Numerical Analysis, Addison-Wesley Co., Massachusetts, 1980.

25. Zienkiewicz, O., The Finite Element Method. McGraw-Hill Book Co., New York, 1977.